

# Simulation of Stress Distribution on Slotted Flap Mechanism Using Finite Element Method

Juan Harris Yedidja Malega<sup>1</sup>, Agus Suprianto<sup>2</sup>, and Muhammad Hadi Widanto<sup>3</sup>

{ malegajuan@gmail.com<sup>1</sup>, agus137@brin.go.id<sup>2</sup>, mhadi@unsurya.ac.id<sup>3</sup> }

Air Marshal Suryadarma Aerospace University, Jakarta 13610, Indonesia<sup>1</sup>  
National Research and Innovation Agency, Bogor 16350, Indonesia<sup>2</sup>  
Air Marshal Suryadarma Aerospace University, Jakarta 13610, Indonesia<sup>3</sup>

**Abstract.** Slotted flaps are one of the most common types of flaps used in aerospace engineering providing significant benefits to aircraft performance during flight phases, by increasing wing area and improving lift force during takeoff and landing. This research paper describes a methodical approach to studying the aerodynamic and structural behavior of a slotted flap mechanism using computer simulations. The process begins with a thorough review of existing literature and the development of a Computer-Aided Design (CAD). Simulations are then conducted using advanced software that combines Computational Fluid Dynamics (CFD) and Finite Element Analysis (FEA). The results from the simulations are seamlessly imported from CAD platform for further analysis. The paper explores four variations of the flight phase. Each with different configurations and velocities and examines their effects on lift distribution and stress tension. The integration of the flap design into the simulation platform allows for precise analysis, including material analysis and load location insights. The central finding of the variations reveals maximum stress results ranging from 135 to 435 Megapascals (MPa), providing valuable insights for optimizing the design in both aerodynamic and structural aspects.

**Keywords:** Stress Distribution, Finite Element, Aerodynamic Characteristic, Slotted Flap

## 1 Introduction

This research paper focus on the design and aerodynamic study of high-lift devices used in aircraft for improved lift characteristics during takeoff and landing [1]. The study aims to provide valuable insights into the intricacies of these devices and their importance in aeronautical engineering. The support structural mechanisms of high-lift devices, including the linkage, lug, and hinges, are critical components that ensure the integrity and functionality of the system. The linkage is designed to transmit motion

and forces, ensuring controlled deployment of high-lift features, while lugs serve as anchor points withstanding dynamic forces. Hinges enable the necessary articulation for adaptive aerodynamic profiles [2]. In previous research on complex multi-hinge flap mechanism, loading was carried out based on aerodynamic considerations [5]. Additionally, research focused on developing flap mechanism designs to enhance the efficiency of flap movement [8]. These component's nuanced design and interaction are essential for the success and safety of high-lift systems. The implementation of slotted flaps contributes to the lift increment achieved by high-lift devices [3]. The slot between the main wing and the flap facilitates controlled airflow, delaying flow separation and reducing drag. Additionally, the creation of a high-energy jet through the flap's trailing edge further enhances lift production. The geometric characteristics of the slotted flap, such as chord length and deflection angle, are influential in shaping aerodynamic forces. Understanding these factors is crucial for optimizing the lift performance of slotted flaps and improving aircraft efficiency during critical phases of flight. Overall, this research paper highlights the significance of high-lift devices in aeronautical engineering and emphasizes the importance of their design and aerodynamic study. By examining the detailed features, design concerns, and aerodynamic complexities, the study aims to contribute to breakthroughs in flight technology and enhance aircraft performance and safety.

## 2 Methods

The research trajectory commences with a diligent exploration of existing literature, establishing a contextual understanding and theoretical groundwork. Subsequently, a meticulous Computer-Aided Design (CAD) is generated, serving as the blueprint for ensuing simulations. These simulations, conducted using advanced simulation software integrating Computational Fluid Dynamics (CFD) and Finite Element Analysis (FEA), provide a virtual arena for scrutinizing the intricacies of the designed system [4]. Following simulation execution, the outcomes are seamlessly imported from the CAD platform, facilitating a seamless transition from design to analysis. Paramount to this process is the definition and input of parameters critical to the simulation's fidelity. The culmination of this methodical approach yields consequential results, notably manifested in the form of aerodynamic loading and stress tension within the slotted flap mechanism. This comprehensive methodology underscores the systematic progression from literature review to simulation outcomes, contributing to a nuanced understanding of the examined system's aerodynamic and structural behavior. In this simulation, there are four variations: [8]

**Table 1.** Variation Flight Phase.

Variation	Flight Level	Flap (Degree)	Velocity (m/s)
1	Cruise	0	58.65
2	Cruise	0	83.85
3	Descent	10	43.73
4	Landing	25	38.6

## 2.1 Computational Fluid Dynamic (CFD)

The synergy between computational fluid dynamics (CFD) and experimental results, particularly in the context of airflow over an airfoil, highlights the effectiveness of CFD as a tool for accurate simulations. The direct analogy drawn between CFD and wind tunnel results demonstrates that CFD can successfully calculate viscous, subsonic, and compressible flow, offering a valuable complement to traditional laboratory experiments. The identification of turbulent flow over the airfoil, supported by consistent results between turbulent CFD simulations and actual experiments, exemplifies the capability of CFD to provide detailed insights beyond basic phenomenological aspects. This case serves as a compelling illustration of the harmonious collaboration between numerical simulations and experimental investigations within the framework of CFD, emphasizing the significant value of such combined approaches in understanding complex fluid dynamics phenomena.

### 2.1.1 Flight profile according to the Load Distribution

At the cruise level with the flaps set at 0 degrees, the lift distribution undergoes a nuanced transformation. At a velocity of 58.65 m/s, the resultant lift is quantified at 142.20, reflecting the system's aerodynamic response. With an increase in velocity to 83.85 m/s, the lift distribution experiences a notable augmentation, reaching 293.83. This velocity-dependent variation in lift distribution underscores the dynamic nature of aerodynamic forces during cruise conditions, with the interplay of velocity and flap configuration significantly influencing lift characteristics. see Fig. 2.

During descent at a configuration with flaps set at 10 degrees and a velocity of 43.73 m/s, the lift distribution assumes a distinct profile. The aerodynamic response at this specific setting yields a lift distribution result of 176.94, highlighting the system's behavior under descent conditions. This numerical representation underscores the intricate relationship between flap configuration, velocity, and the resultant lift forces during the descent phase, providing valuable insights into the aerodynamic characteristics of the aircraft. At the landing phase with flaps extended to 25 degrees and a velocity of 38.6 m/s, the lift distribution undergoes a substantial transformation. The aerodynamic forces at play manifest in a lift distribution result of 241.79, reflecting the impact of both the increased flap angle and reduced velocity characteristic of the landing configuration. This nuanced interplay between flap deployment, airspeed, and resulting lift distribution provides critical insights into the aerodynamic behavior crucial for a safe and controlled landing. see Fig. 3.

Wing sections 1-6 are uniformly spaced at a distance of 412.5 mm each, ensuring consistent and systematic distribution along the wing structure. The utilization of the position model for the inner wing plays a pivotal role in the Finite Element Method (FEM) simulation. The inner wing, housing a complex flap mechanism comprised of a Lug, linkage, and pin, is integral to the overall structural dynamics. In this simulation, the focus is primarily on the inner wing due to its direct involvement in the intricate linkage mechanism. The detailed position model of the inner wing captures the precise spatial relationships between its components, providing essential data for the FEM simulation. Conversely, the outer wing, devoid of such a linkage mechanism, is excluded

from active participation in the simulation as its structural contributions are deemed insufficient. This targeted approach ensures that the simulation accurately reflects the mechanical behavior influenced by the flap mechanism, offering engineers a nuanced understanding of the inner wing's role in the broader structural dynamics. see Fig. 4.

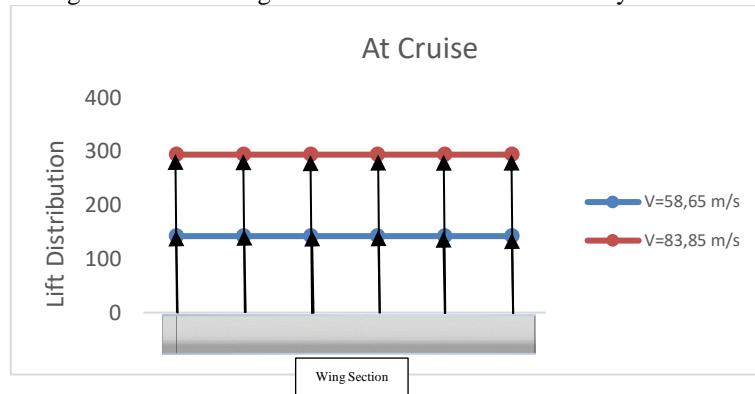


**Fig. 1** Lift distribution at Cruise chart

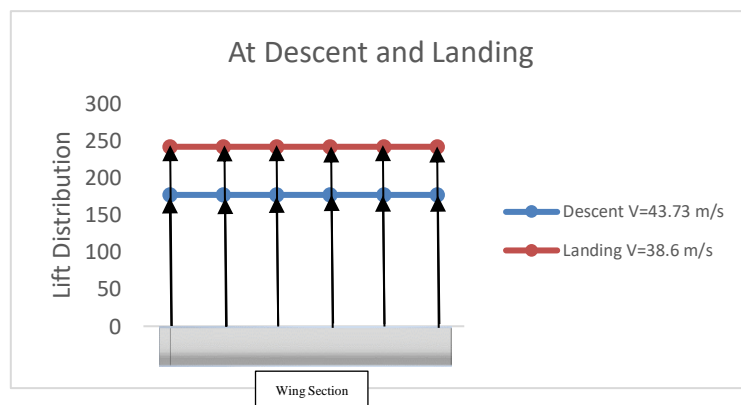


**Fig. 2** Lift distribution at Descent and Landing chart

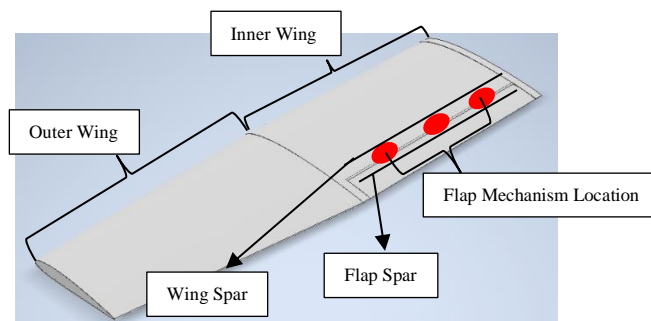


**Fig. 3** Wing platform name selection

### 2.1.2 Result CFD Simulation

The CFD post-processing results for Variations 1 to 4, each with distinct aircraft velocity, are visually represented through contour plots focusing on pressure distribution. In Variation 1, where the velocity is 58.65 m/s, the contour pressure plot illustrates the dynamic pressure patterns across the object's surface. Variation 2, with a higher velocity of 83.85 m/s, showcases how increased velocity influences and intensifies the pressure distribution, providing valuable insights into the aerodynamic forces at play. Contrastingly, Variation 3, with a reduced velocity of 43.73 m/s, exhibits pressure contours that reflect the nuanced aerodynamic interactions under slower conditions. Finally, Variation 4, with velocity speed of 38.6 m/s, emphasizes the effect of reduced velocity on pressure distribution, highlighting specific regions subjected to varying degrees of aerodynamic forces. These contour pressure plots, tailored to each variation's air flow speed, serve as critical visual tools for engineers to comprehend the intricate relationship between velocity, pressure, and structural response in the pursuit of optimizing overall performance. See Fig. 4, 5, 6, 7.

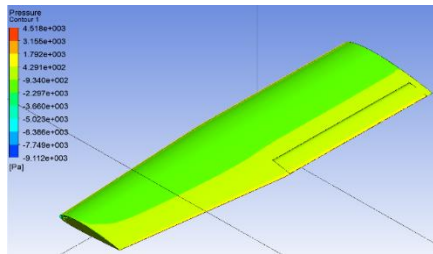


Fig. 4 Contour Pressure at 58.65 m/s

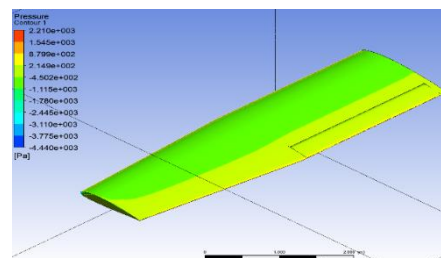


Fig. 5 Contour Pressure at 83.85 m/s

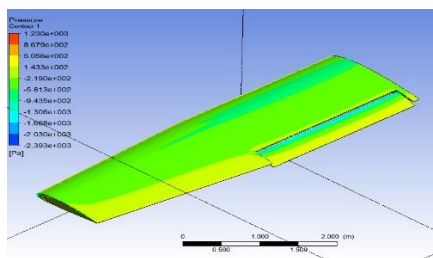


Fig. 6 Contour Pressure at 43.73 m/s

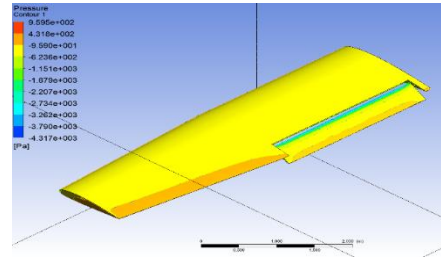


Fig. 7 Contour Pressure at 38.6 m/s

## 2.2 Finite Element Analysis (FEA)

### 2.2.1 Model and Material Import

The design of the flap mechanism's motion is integrated into the MotionView simulation platform. The model utilizes millimeters for length, Newtons for force, seconds for time, and kilograms for mass in its unit system. Key moving components of the flap mechanism, including the Wing rear spar, flap mechanism (lug, linkage, and pin), and Flap front spar, are retained in the simulation [5]. see Fig. 9.

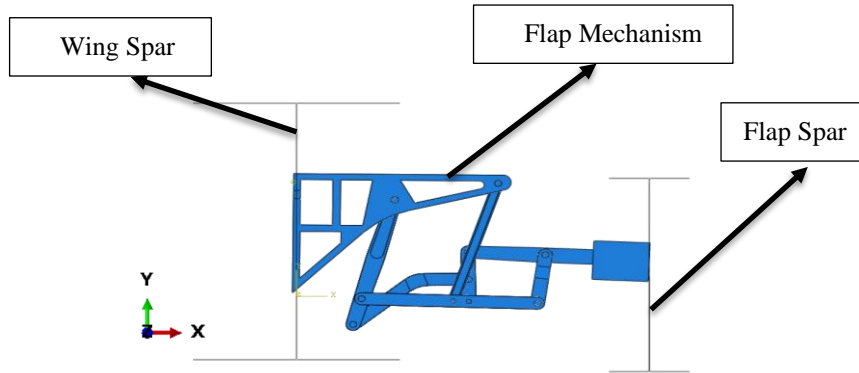


Fig. 8 2D view model.

The flap mechanism parts are constructed from Aluminum Alloy 7050-T73, while the spars are composed of Aluminum Alloy 2024-T42 [7]. see Table 2.

Table 2. Material Properties. [6][10]

Material	Density (Tonne/mm <sup>3</sup> )	Young's Modulus (MPa)	Poisson Ratio	Yield Stress (MPa)	Ultimate Tensile Strength (MPa)
AA 2024-T42	2.77e-09	72400	0.33	300	470
AA 7050-T73	2.81e-09	72000	0.33	435	550

### 2.2.2 Boundary Condition

In this case, fixed boundary conditions are applied to the end of the wing root attached to the fuselage. see Fig. 13. In the context of boundary conditions, it also applies to the lug parts that attach to the wing spars, emphasizing the interconnected influence of structural elements on overall system behavior. see Fig. 14.



**Fig. 13** Boundary condition location

In the context of boundary conditions, it also applies to the lug parts that attach to the wing spars, emphasizing the interconnected influence of structural elements on overall system behavior.

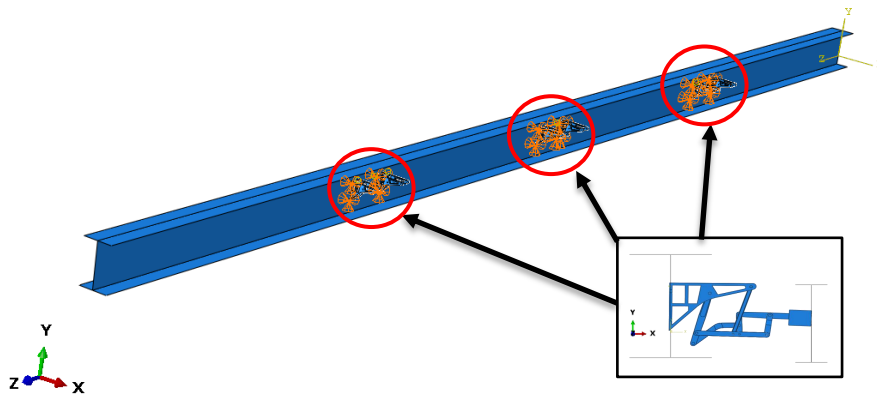


**Fig. 14** Location of Boundary condition at Lug

### 2.2.3 Load Pressure

The results of the CFD simulation have provided valuable insights into the location of loads on both the wing spar and flap spar. The aerodynamic forces acting on the wing structure have been meticulously analyzed, revealing critical points where these forces exert their influence. The contour plots generated from the CFD data precisely indicate the distribution of loads along the surface of the wing spar, elucidating areas experiencing significant aerodynamic pressures. Simultaneously, the flap spar, housing the intricate flap mechanism, is also subjected to distinct load patterns discerned from the simulation results. Engineers can leverage this information to understand not only the overall distribution of forces on the wing but also the nuanced mechanical responses of specific components like the flap spar. This detailed knowledge is paramount for optimizing structural design, ensuring appropriate reinforcement of materials in regions prone to high aerodynamic pressures, and ultimately enhancing the overall performance and reliability of the wing system. see Fig. 9,10,11,12.

**Cruise condition**

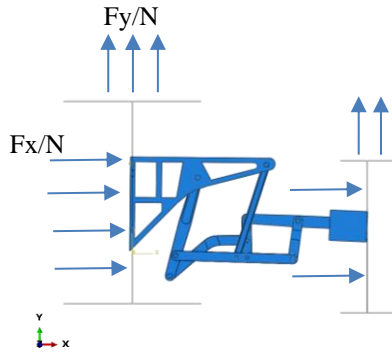


**Fig. 9** Load location at Variation 1

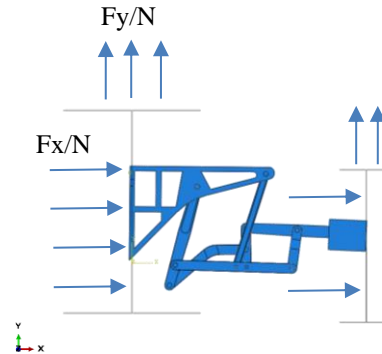


**Fig. 10** Load location at Variation 2

**Descent condition**

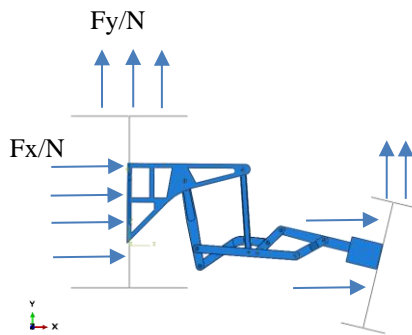


**Fig. 11** Load location at Variation 3

**Landing condition**

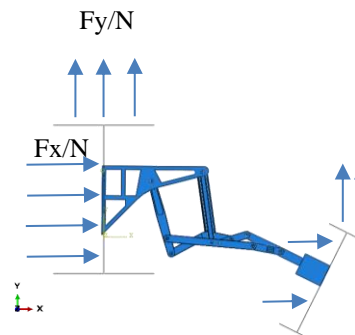


**Fig. 12** Load location at Variation 4

The CFD simulation results reveal precise loading locations on the wing spar and flap spar, offering critical insights into the distribution of aerodynamic forces and facilitating strategic structural optimizations for enhanced performance. see Table 3.

**Table 3.** Applied Load [5].

Variation	Wing spar	Wing Spar	Flap Spar	Flap Spar
	Fx/N	Fy/N	Fx/N	Fy/N
1	173.945	142.202	31.6277	52.89
2	350.687	293.831	67.89	110.732
3	186.865	176.937	6.401	138.017
4	297.145	241.796	55.765	201.364

### 2.2.4 Mesh

The following is the input data for the meshing process which is treated in 12 component parts.

**Table 4.** Total Mesh

Name Part	Element Size (mm)	Element Part	Piece	Total Element/Part
Part 11	0.5	5557	12	66684
Part 15	0.5	5624	12	67488
Part 20	0.5	1701	24	40824
Part 21	0.5	762	12	9144
Part 25	0.5	4882	6	29292
Part 30	0.5	38292	6	229752
Part 40	0.5	3404	6	20424
Part H1	0.5	13686	12	164232
Pin D2T5	0.2	748	12	8976
Pin D2T7	0.2	3360	48	161280
Pin D2T8	0.2	3840	6	23040
Pin D2T16	0.2	7680	6	46080
Pin D14T3	0.2	900	12	10800
Pin D14T7	0.2	2100	12	25200
Wing Spar	10	5520	1	5520
Flap Spar	10	2550	1	2550
<b>TOTAL</b>				<b>911286</b>

## 3 Result and Discussion

From several FEA simulation variations, the stress results caused by the simulation of aerodynamic loading using CFD simulations were obtained.

### 3.1 Condition at Variation 1

The outcomes of the finite element method simulation reveal a critical finding regarding the continuous safety factor, with the pin component exhibiting the highest stress point at 135.3 MPa. see Fig. 15 and Fig. 16

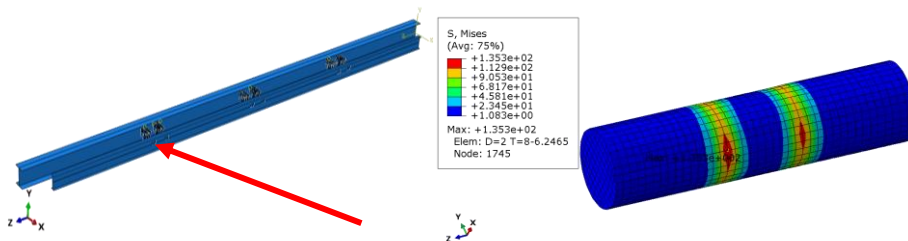


**Fig. 15** Location Maximum Stress Variation 1 **Fig. 16** Maximum Stress Contour at Variation 1

### 3.2 Condition at Variation 2

The findings from the finite element method simulation reveal that within the analyzed structural system, the pin component bears the most significant stress, registering at 286.1 Megapascals.

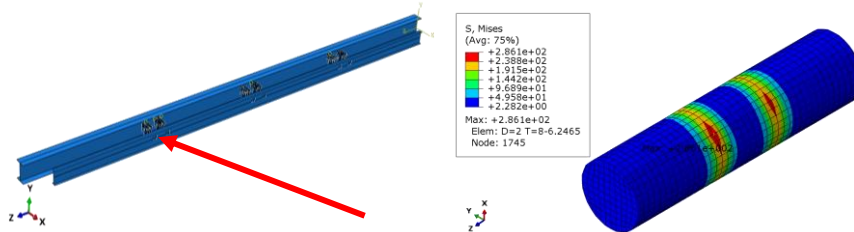


**Fig. 17** Location Maximum Stress Variation 2 **Fig. 18** Maximum Stress Contour at Variation 2

### 3.3 Condition at Variation 3

The outcomes derived from the finite element method simulation reveal that the pin component exhibits the highest stress concentration, peaking at 313.8 megapascals (MPa). see Fig. 19 and Fig. 20

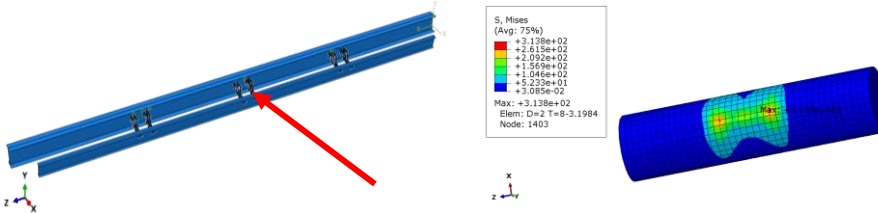


**Fig. 19** Location Maximum Stress Variation 3 **Fig. 20** Maximum Stress Contour at Variation 3

### 3.4 Condition at Variation 4

The outcomes of the finite element method simulation reveal that within the analyzed structure, the pin component experiences the highest stress concentration, reaching a critical value of 435 megapascals.

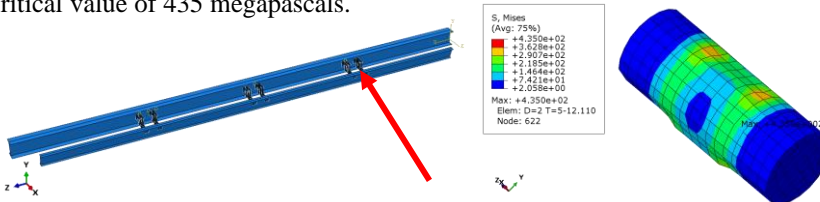


**Fig. 21** Location Maximum Stress Variation 4 **Fig. 22** Maximum Stress Contour at Variation 4

### 3.5 Factor of Safety

The greater the Factor of Safety (FoS), the more secure the product or structure becomes. An FoS of 1 signifies that a structure or component will immediately fail when subjected to the design load, incapable of supporting any additional load. Structures or components with a FoS below one are deemed unacceptable. In cases where failure consequences are severe, leading to potential loss of life or physical injury, a higher FoS is mandated either through design considerations or legal requirements. [9]

Factor Safety Equation:

$$\text{Factor of Safety} = \frac{\text{Ultimate Tensile Strength (MPa)}}{\text{Working or design stress (MPa)}} \quad (1)$$

Result FoS Flap Mechanism based on equation (1). The following are the results of the safety factor calculation. see Table 4.

**Table 5.** Result Factor of Safety Design Flap Mechanism.

Variation	Ultimate Strength (MPa)	Design Stress (MPa)	Factor of Safety
1	550	135	4.07
2	550	286.1	1.92
3	550	313.8	1.75
4	550	435	1.26

## 4 Conclusion

In conclusion, the investigation into lift distribution during descent and landing highlights the significant influence of flap angle and velocity on the aerodynamic characteristics of the slotted flap mechanism. The observed lift distributions at different configurations provide valuable insights into the behavior of the system under specific conditions, shedding light on the intricate interplay between flap settings and flight phases. Furthermore, the integration of flap mechanism design with structural analysis, as presented in this study, offers a comprehensive approach to optimize the structural design and enhance the safety and performance of the slotted flap mechanism.

Moreover, the mechanical response and stress distribution analysis reveal critical information about the material system's behavior under varying conditions. The varying stress values across different design variations underscore the importance of considering the structural implications of different configurations. The Factor of Safety (FoS) assessment further contributes to the overall understanding, with Variations 1 and 2 exhibiting robust safety margins, while Variations 3 and 4 suggest a need for careful consideration and potential design modifications to ensure optimal safety, particularly in scenarios where failure consequences are critical. This research paper thus provides a thorough methodology for studying both aerodynamic and structural aspects, making a valuable contribution to the field of slotted flap mechanism design and analysis.

## References

1. Lima, D. Zilli., F. Wallace., Aguiar, J. Batista: Preliminary Structural Design of Fowler Flap High-Lifting Device (2021).
2. Zaccai, D., Bertels, F., Vos, R.: Design methodology for trailing-edge high-lift mechanism. CEAS Aeronaut J, 7:521-534 (2016).
3. Hussein, E.Q., Azziz, H. N., Rashid, F. L.: Aerodynamic study of slotted flap for NACA 24012 Airfoil by Dynamic mesh techniques and visualization flow. Journal of Thermal Engineering, Vol.7, No.2, 13 pp. 230-239. (2021).
4. Beker, C., Turgut, A. E., Arikan, K. B., Kurtulus, D. F: Fluid-Structure Interaction Analysis of a Four-Bar Flapping Wing Mechanism (2019)
5. Feng, Y., He, Z., Xue, X., Dong, M.: Dynamic simulation of complex multi-hinge space flap mechanism. In: The 12<sup>th</sup> Asia Conference on Mechanical and Aerospace Engineering, pp. 3-4. IOP Publishing, (2022).
6. <https://asm.matweb.com/search/SpecificMaterial.asp?bassnum=ma7075t73>, last accessed 2023/09/07.
7. Cessna Aircraft Company.: Single Engine Structural Repair Manual. Revision 4, USA (2005)
8. Feng, Y., He, Z., Xue, X., Dong, M.: Design of flap/spoiler follower mechanism for civil aircraft. In: The 13<sup>th</sup> Asia Conference on Mechanical and Aerospace Engineering, pp. 3-6. IOP Publishing, (2023)
9. <https://safetyculture.com/topics/factor-of-safety/>, last accessed 2023/24/10.
10. <https://www.makeitfrom.com/material-properties/2024-T42-Aluminum>, last accessed 2023/09/07
11. Anderson, J.: Computational Fluid Dynamics The basic with Applications. 1<sup>st</sup> edn. McGraw-Hill, Inc. United States of America (1995).